ИНСТИТУТ ЯДЕРНОЙ ФИЗИКИ СО АН СССР

V.M.Aulchenko, S.I.Dolinsky, V.P.Druzhinin, M.S.Dubrovin,
S.I.Eidelman, E.S.Gluskin, V.B.Golubev, V.N.Ivanchenko,
P.M.Ivanov, G.Ya.Kezerashvili, I.A.Koop,
A.P.Lysenko, A.A.Mikhailichenko, E.V.Pakhtusova,
E.A.Perevedentsev, A.N.Peryshkin, A.A.Polunin, I.Yu.Redko,
S.I.Serednyakov, V.A.Sidorov, A.N.Skrinsky, A.S.Sokolov,
Yu.M.Shatunov, I.B.Vasserman, P.V.Vorobyov, Yu.V.Usov

STUDY OF DECAYS OF ρ AND ω-MESONS WITH THE NEUTRAL DETECTOR AT THE VEPP-2M COLLIDER

PREPRINT 86-105

НОВОСИБИРСК
1986

ABSTRACT

Preliminary results of experiments with the Neutral Detector at the electron-positron collider VEPP-2M are presented for the c.m. energy range 500—1000 MeV. The ω-meson total width have been measured:

$\Gamma_\omega = 8.52 \pm 0.16$ MeV

Its value is by 15% less than the table value. Branching ratios of the ρ and ω-meson decays have been measured:

$B(\omega \to 3\pi) = 0.896 \pm 0.008$,
$B(\omega \to \pi^0\gamma) = 0.090 \pm 0.008$,
$B(\omega \to \eta\gamma) = (4.6^{+3.8}_{-2.2}) \cdot 10^{-4}$,
$B(\omega \to e^+e^-) = (7.2 \pm 0.5) \cdot 10^{-5}$,
$B(\rho \to \pi^0\gamma) = (7.9 \pm 3.5) \cdot 10^{-4}$,
$B(\rho \to \eta\gamma) = (4.5 \pm 1.7) \cdot 10^{-4}$.

The branching ratio of the decay $\rho \to \pi^+\pi^-\gamma$ has been measured for the first time:

$B(\rho \to \pi^+\pi^-\gamma) = 0.013 \pm 0.002$

at the photon energy more than 50 MeV. It has been shown that bremsstrahlung radiation of pions dominates in this decay. The upper limit for the probability of direct photon emission has been placed:

$B(\rho \to \pi^+\pi^-\gamma) < 7 \cdot 10^{-4}$ 90% confidence level.

The upper limit for the branching ratio is:

$B(\omega \to \pi^0\pi^0\gamma) < 5 \cdot 10^{-4}$ 90% confidence level.

1. INTRODUCTION

Radiative transitions between the vector and pseudoscalar mesons provide important information on the hadron structure and their properties. In these reactions the quark contents of the meson does not change, and a spin of one of the quarks flips. The probabilities of different radiative decays are related to each other through SU(3), quark model and vector dominance model (VDM) (cf. the review paper [1]). They are also related to the probabilities of two-photon decays of pseudoscalar mesons and the values of baryon magnetic moments. Eleven such transitions exist for the mesons consisting of light quarks, most of them being already measured [2]. However, the measurement accuracy is not sufficient for a detailed check of theoretical predictions.

The great number of experimental works is devoted to the investigation of the decay $\omega \to \pi^0\gamma$. Its value is used as a normalization in various experimental and theoretical studies. Different techniques were applied to measure this decay width [2]. The highest relative accuracy attained in a single experiment is 15% [3], whereas the error of the world average value obtained by averaging all available results is 5% [2]. However, in Ref. [4] most of the experiments on $\omega \to \pi^0\gamma$ determination were criticised, since they assumed the decay $\omega \to \pi^0\gamma$ to be the only neutral decay mode of the ω-meson. This emphasizes the importance of the new high precision measurement of this quantity. The other radiative decays of the ρ and ω mesons are known with much worse accuracy.

Note that radiative decays of ϱ and ω mesons were earlier studied mostly in fixed target experiments. e^+e^--collisions provide a source of ϱ and ω meson free of background. However, the statistical accuracy of the previous e^+e^- experiments [5] was relatively low because of the small integrated luminosity. The VEPP-2M collider [6] has the highest luminosity in the c.m. energy range below 1.4 GeV. The installation of the wiggler magnet allowed an increase in the luminosity in the energy range of ϱ and ω mesons [7]. At the present time an experiment is in progress at VEPP-2M in the c.m. energy range 500—1000 MeV aimed at the study of radiative decays with the Neutral Detector [8]. It is planned to collect an integrated luminosity of about 5 pb^{-1}.

The main part of the detector is an electromagnetic calorimeter consisting of 168 NaI(Tl) crystals with a total weight of 2.5 tons. Earlier this detector was used to study the radiative decays of the Φ-meson [9] and hadron production in the energy range 1.0—1.4 GeV. In this work we present the preliminary results using an event sample corresponding to the integrated luminosity of 1.2 pb^{-1}. The experiment was performed at the average luminosity of $0.5\cdot10^{30}$ $cm^{-2}sec^{-1}$. The number of recorded events was $4.6\cdot10^6$ of which $4\cdot10^5$ were due to the ω-meson decays and 10^6 to those of ϱ-mesons.

Great attention was paid to the determination of the ω-meson parameters, in particular its total width Γ_ω and partial width $\Gamma(\omega\to e^+e^-)$. To this end besides radiative decays a dominant decay mode $\omega\to3\pi$ has also been studied.

2. DECAY $\omega\to3\pi$

To study the process

$$e^+e^-\to\omega\to\pi^+\pi^-\pi^0 \qquad (2.1)$$

data obtained in the scan of the energy range $2E=740-814$ MeV were used corresponding to the integrated luminosity of 0.9 pb^{-1}. Events were selected with two charged particles and two photons presumably from the π^0-meson decay. It was also required that the minimum angle between the particles in an azimuthal plane be greater than 30°. This cut suppressed the background due to the processes $e^+e^-\to e^+e^-$, $\pi^+\pi^-$ and decreased a systematic error in the

detection efficiency due to the uncertainty in the simulation of nuclear interactions of pions with the detector material. The detection efficiency of the process (2.1) was energy independent and was 4%. About $1.3\cdot10^4$ events have been found satisfying these criteria.

In Fig. 1 the distribution in the invariant mass of two photons is shown for experimental events at $2E=782$ MeV and for Monte Carlo events of the process (2.1). It can be seen that the main contribution to the observed events comes from the reaction (2.1). In Fig. 2 we show the detection cross section of selected events. Normalization used the events of Bhabha scattering and had a 3% accuracy.

The decay mode $\varrho\to\pi^+\pi^-\pi^0$ violating G-parity can distort the cross section due to the interference with the process $\omega\to\pi^+\pi^-\pi^0$. The probability of this decay is estimated to be

$$B(\varrho^0\to\pi^+\pi^-\pi^0)=B(\omega\to\pi^+\pi^-\pi^0)\cdot B(\omega\to\pi^+\pi^-)\left(\frac{\Gamma_\omega}{\Gamma_\varrho}\right)^2\approx5\cdot10^{-5}$$

Since this value is small the decay mode $\varrho\to\pi^+\pi^-\pi^0$ was not taken into account. In the energy range under study the effect of ω—Φ interference is negligible. Therefore the cross section of (2.1) can be written as

$$\sigma(e^+e^-\to\pi^+\pi^-\pi^0)=\sigma_0\frac{M_\omega^2\Gamma_\omega^2}{(S-M_\omega^2)^2+S\Gamma_\omega^2(S)}\cdot\frac{F(S)}{F(M_\omega^2)}(1+\delta_R) \qquad (2.2)$$

where σ_0 is the cross section value in the resonance peak, M_ω, Γ_ω are the resonance mass and width, $F(S)$ is a factor taking into account the $\omega\to\varrho\pi\to3\pi$ transition [11], δ_R is a radiative correction calculated according to Ref. [12].

The energy dependence of the total width was parametrized as follows

$$\Gamma_\omega(S)=\Gamma_\omega\frac{S^{3/2}}{M_\omega^3}\frac{F(S)}{F(M_\omega^2)}$$

ω-meson parameters were determined by a maximum likelihood method using the table values of the ω-meson mass [2]. Four parameters were determined in the fit: the ω-meson width, peak cross section σ_0, a level of nonresonant background and a shift of the energy scale of the collider. The last parameter was introduced because absolute calibration of the collider energy scale was not performed.

Taken into account were the beam energy spread of 0.17 MeV, the accuracy of the beam energy setting of 0.05 MeV as well as the statistical error of the integrated luminosity.

In Fig. 2 we show an optimal curve corresponding to the following values of the parameters ($P(\chi^2)=70\%$):

$$\Gamma_\omega = 8.52 \pm 0.16 \text{ MeV} \tag{2.3}$$

$$\sigma_0 = 1.54 \pm 0.03 \pm 0.12 \text{ μb} \tag{2.4}$$

The level of nonresonant background was about 1% of the detection cross section in the peak. The first error is statistical, while the second one is systematic due to the restricted number of the Monte Carlo events and the uncertainty in the simulation of nuclear interaction of pions with the detector material.

To check the reliability of the obtained result data processing was repeated with different selection criteria. Within the errors the results (2.3) and (2.4) did not change. Additionally we have done data processing for events with two charged particles and only one photon from the π^0 meson decay. The obtained results are statistically consistent with the values above.

3. DECAY $\varrho \to \pi^+\pi^-\gamma$

Two different mechanisms contribute to the radiative decay $\varrho \to \pi^+\pi^-\gamma$: pion bremsstrahlung in the decay $\varrho \to \pi^+\pi^-$ and direct photon emission connected with the rearrangement of the quark structure in the decay of ϱ-meson, for example, a possible electric dipole transition $\varrho \to \varepsilon\gamma$. Since the decay $\varrho \to \pi^+\pi^-$ is dominant for the ϱ-meson, the bremsstrahlung mechanism must be important. Its probability was calculated in Refs [13—15] and equaled about 10^{-2} at the photon energy higher than 50 MeV. The second mechanism was considered in Ref. [15] taking into account transitions through intermediate f, A_1, A_2-mesons as well as possible $\sigma(400)$ and $\varepsilon(700)$ scalar resonances. A transition through a scalar resonance can dominate, e. g. for the decay $\varrho \to \varepsilon(700)\gamma$ the value $1.7 \cdot 10^{-4}$ was obtained. Direct emission can be observed by the difference in the shape of the photon energy spectrum from the bremsstrahlung case.

The same final state is produced in the reaction $e^+e^- \to \varrho\gamma$ when a photon is emitted by initial particles. However, because of the different C-parity of the $\pi^+\pi^-$ system these processes do not interfere

(pion signs in the experiment are not distinguished) and the cross section of the reaction $e^+e^- \to \pi^+\pi^-\gamma$ can be written as

$$\sigma_{e^+e^-\to\pi^+\pi^-\gamma} = \sigma_{e^+e^-\to\varrho\gamma} + \sigma_{\varrho\to\pi^+\pi^-\gamma}$$

The cross section of the process $e^+e^- \to \varrho\gamma$ can be calculated with high accuracy in quantum electrodynamics [14, 16] using the well-known cross section $\varrho \to \pi^+\pi^-$.

To study the process $e^+e^- \to \pi^+\pi^-\gamma$ events were selected with two charged particles and one photon producing a spark in shower chambers. Also required was energy-momentum balance. To suppress the background due to the process $e^+e^- \to e^+e^-\gamma$ the procedure of e/π separation was used [17]. The distribution in the separation parameter is shown in Fig. 3, where the lines correspond to the boundary between π and e. The number of remaining events of the process $e^+e^- \to e^+e^-\gamma$ was estimated from the same distribution and did not exceed 2—5% in the energy range 500—200 MeV. Selected events can be due to one of the four processes:

$$e^+e^- \to \varrho \to \pi^+\pi^-\gamma \tag{3.1}$$

$$e^+e^- \to \varrho\gamma \to \pi^+\pi^-\gamma \tag{3.2}$$

$$e^+e^- \to \mu^+\mu^-\gamma \tag{3.3}$$

$$e^+e^- \to \pi^+\pi^-\pi^0 \tag{3.4}$$

In the ω-meson region the cross section of the process (3.4) dominates and its value is determined by the excitation curve of the ω-meson. To approximate the cross section (3.4) ω—Φ interference was taken into account (formula (2.2)). Energy dependence of the detection efficiency was determined from the simulation. The contribution of (3.2) and (3.3) was calculated and subtracted. A systematic uncertainty in the simulation of these processes was estimated to be 10%. Selected events were divided into five groups according to the photon energy and in each group the background due to the processes (3.2—3.4) was subtracted. The photon energy spectrum thus obtained is presented in Fig. 4. Also shown there is the photon spectrum for the bremsstrahlung mechanism under the same selection criteria. The figure shows that the direct emission does not give a significant contribution. Therefore one can obtain the probability of the bremsstrahlung mechanism and place an upper limit for the contribution of the direct emission.

The energy dependence of the detection cross section for selected

events (background from the reaction (3.4) subtracted) is shown in Fig. 5 for $E_\gamma > 50$ MeV. The following formula was used in the approximation:

$$\sigma_{vis} = \alpha\sigma_1 + \sigma_2 + \sigma_3,$$

where σ_1 is the calculated cross section of the process (3.1) proceeding through the bremsstrahlung mechanism, σ_2 and σ_3 are the calculated detection cross sections for the processes (3.2) and (3.3), α is a free parameter allowing for the difference between the experimental cross section and the calculated one. The contribution of all three processes as well as the sum of the detection cross sections are presented in Fig. 5. For α the following value was obtained:

$$\alpha = 1.20 \pm 0.10 \pm 0.15.$$

The first error is statistical and the second one is systematic and due to the systematics of Monte Carlo simulation. Experimental points are in good agreement with the bremsstrahlung mechanism. For the peak cross section and the branching ratio the following values have been obtained:

$$\sigma_0(\varrho \to \pi^+\pi^-\gamma) = 15 \pm 3 \text{ nb},$$

$$B(\varrho \to \pi^+\pi^-\gamma) = (1.3 \pm 0.2)\%$$

at $E_\gamma > 50$ MeV (bremsstrahlung mechanism). To place a limit for the probability of the direct emission write the matrix element for the decay $\varrho \to \pi^+\pi^-\gamma$ in the following form:

$$M = M_b + M_i,$$

where M_b is the matrix element for bremsstrahlung, M_i is the matrix element for direct emission. As shown in Refs [13, 14], it is proportional to the first power of the photon momentum and distorts a hard part of the photon spectrum. For a transition through a scalar resonance the matrix element can be written as

$$M_i^S = \frac{Ae^{i\theta}}{S_1 - M^2 - iM\Gamma} \cdot [(pk)g_{\mu\nu} - p_\mu k_\nu] e_\nu^{(\varrho)} e_\mu^{(\gamma)},$$

where S_1 is an invariant mass of the $\pi^+\pi^-$ pair, M and Γ are mass and width of the scalar resonance, p and k are momenta of ϱ-meson and photon, $e^{(\varrho)}$, $e^{(\gamma)}$ are their polarizations, A and θ are the absolute value and the phase of the complex amplitude of the transition $\varrho \to \varepsilon\gamma \to \pi^+\pi^-\gamma$. In Fig. 4 the spectrum due to the direct emission is shown for $M = 700$ MeV and $\Gamma = 100$ MeV. The spectrum differs notably from the bremsstrahlung case. The resulting spectrum must take into account the interference of two mechanisms. Therefore in the fit the phase θ was a free parameter. Two possible intermediate states were considered: scalar resonances $\sigma(400)$ and $\varepsilon(700)$ with a width of 100 MeV. The following limits were placed:

$$B(\varrho \to \sigma(400)\gamma) < 1 \cdot 10^{-4},$$

$$B(\varrho \to \varepsilon(700)\gamma) < 7 \cdot 10^{-4}, \quad 90\% \text{ c.l.}$$

Since the photon spectrum is well described by the bremsstrahlung mechanism and the contribution of the direct emission is small, the expression for M_i^S is adequate for the description of direct emission for any intermediate state. Thus for the branching ratio of the direct emission the following limit is obtained:

$$B(\varrho \to \varepsilon\gamma) < 7 \cdot 10^{-4} \quad 90\% \text{ c.l.}$$

4. PROCESSES $e^+e^- \to \pi^0\gamma$, $\eta\gamma$, 3γ.

The radiative decays have been investigated in the reactions:

$$e^+e^- \to \varrho, \ \omega \to \pi^0\gamma, \quad \pi^0 \to 2\gamma, \tag{4.1}$$

$$e^+e^- \to \varrho, \ \omega \to \eta\gamma, \quad \eta \to 2\gamma. \tag{4.2}$$

The recoil photons in these reactions are monochromatic. This allows a separation of these reactions between each other and from the following quantum electrodynamic process:

$$e^+e^- \to 3\gamma. \tag{4.3}$$

For selection of three-photon events due to the processes (4.1—4.3) a kinematical fit has been used. The background caused by two-quantum annihilation was removed by the following requirements: an angle between any two photons is greater than 28°, an energy of any photon is less than $0.985E$. The Dalitz plot of the selected 3841 events is shown in Fig. 6. This figure also shows the distribution of events for the processes (4.1—4.3) obtained by simulation. Events of radiative decays are concentrated on the diagram

around the lines corresponding to the energies of the recoil photons in these decays:

$$\omega_P = E\,[1-(M_P/2E)^2], \tag{4.4}$$

where M_P is a pseudoscalar meson mass. ω_P depends on the beam energy E, therefore it is convenient to use in the further analysis the following parameter:

$$D_{iP} = (\omega_i - \omega_P)/E, \tag{4.5}$$

where ω_i $(i=1, 2, 3)$ is the photon energy $(\omega_1 > \omega_2 > \omega_3)$. In the energy range of the ω-meson the recoil photon in most of the events has the maximum energy $(i=1)$ in an event of the reaction (4.1) and the minimum energy $(i=3)$ in an event of the reaction (4.2). The clear peak is observed in the distribution over $D_{1\pi}$ (Fig. 7). It shows that background due to the process (4.3) is small. For further analysis of the cross sections the following criteria have been used: $|\min_i D_{i\pi}| < 0.015$ for selection of the process (4.1) and $|D_{i\pi}| > 0.045$ for selection of the processes (4.2) and (4.3). The small peak in the distribution over $D_{3\eta}$ (Fig. 8) is connected with events of the reaction (4.2). These events were selected by the condition $|\min_i D_{i\eta}| < 0.05$.

In order to fit the experimental data, the detection cross sections were written as follows:

$$\sigma_{vis}(S) = \sigma_{\pi^0\gamma}(S) + \sigma_{\eta\gamma}(S) + \sigma_{3\gamma}(S),$$

$$\sigma_{P\gamma}(S) = \sigma_{TP\gamma}(S) \cdot \varepsilon_{P\gamma}(S) \cdot \lambda_{P\gamma}(S),$$

$$\sigma_{3\gamma}(S) = k(S) \cdot \sigma_{03\gamma} \cdot \frac{800^2}{S},$$

$$\sigma_{TP\gamma}(S) = |A_\omega + A_\varrho e^{i\theta_\varrho} + A_\Phi e^{i\theta_\Phi}|^2,$$

$$A_V = \frac{\sqrt{\sigma_0(V\to P\gamma)}\, M_V \Gamma_V}{M_V^2 - S - i\sqrt{S}\,\Gamma_V(S)} \left(\frac{1-M_P^2/S}{1-M_P^2/M_V^2}\right)^{3/2}, \tag{4.6}$$

where σ_{vis} are the detection cross sections, $\sigma_{TP\gamma}$ are the calculated cross sections, $\varepsilon_{P\gamma}$ are the detection efficiencies (Table 1), $\lambda_{P\gamma}$ is a factor taking into account radiative corrections and beam energy spread, $\sigma_{03\gamma}$ is the detection cross section for the process (4.3) for $E=400$ MeV, k is a coefficient taking to account different contributions of the process (4.3) into visible cross sections of the proces-

ses (4.1) and (4.2) (Table 1), A_V is a Breit-Wigner amplitude taking into account phase space, $\sigma_0(V\to P\gamma)$ are the cross sections in the resonance maximum, θ_V are relative phases of the ω—ϱ and ω—Φ interference.

The detection efficiencies were calculated taking into account the radiative corrections. They depend on the beam energy because of a smaller efficiency of shower chambers to low energy photons.

Table 1

Detection Efficiency and Values of the Coefficient k for the Beam Energy $E=391$ MeV

Selection criteria	$\varepsilon_{\pi^0\gamma}$ (%)	$\varepsilon_{\eta\gamma}$ (%)	k
$\pi^0\gamma$	9.0 ± 0.3	0.5 ± 0.1	0.77 ± 0.13
$\eta\gamma$	<0.02	3.1 ± 0.2	0.43 ± 0.17
3γ	$(1.6\pm1.1)\cdot10^{-2}$	0.90 ± 0.05	1.00 ± 0.09

As a result of fitting the data for the process (4.3) the value of the cross section has been obtained $\sigma_{03\gamma} = (0.219\pm0.015)$ nb, which is in good agreement with the calculated value (0.205 ± 0.010). Thus the contribution of any nonresonant processes to visible cross sections is negligibly small.

The energy dependence of the cross sections for the reactions (4.1) and (4.2) is determined by interference of the ϱ- and ω-mesons. Because of its small mass difference $(M_\omega - M_\varrho) \ll \Gamma_\varrho$, good fit of the data may be achieved both at the constructive and destructive interference. Formally this means that the likelihood function has two minima: one of them near the value of the interference phase $\theta_\varrho = 0°$, another—near $\theta = 180°$. Therefore fit has been done twice with two different initial values of this phase θ_ϱ. In the fit we used cross sections $\sigma_0(\Phi\to P\gamma)$ which have been obtained in our previous work [9], the table values of the meson masses and a value of the interference phase $\theta_\Phi = 180°$.

As free parameters of the fit for the reaction (4.1) we have chosen $\sigma_0(\omega\to\pi^0\gamma)$, $\sigma_0(\varrho\to\pi^0\gamma)$, and Γ_ω. The following value of the total width of the ω-meson has been obtained $\Gamma_\omega = (8.2\pm0.3)$ MeV, which is consistent with (2.3), but has a larger error. This allows to fit the data using the value (2.3) (Table 2).

Table 2

Results of the Fitting the Cross Section of the Reaction $e^+e^- \to \varrho, \omega \to \pi^0\gamma$

Parameters of the fit	$\theta_\varrho \sim 180°$	$\theta_\varrho \sim 0°$
$\sigma_0(\omega \to \pi^0\gamma)$ (nb)	243 ± 7	154 ± 7
$\sigma_0(\varrho \to \pi^0\gamma)$ (nb)	6.2 ± 0.9	0.9 ± 0.4
θ_ϱ (deg)	165 ± 2	-5 ± 6
χ^2/n_D	38/45	38/45

Only statistical errors are given in Table 2. A systematic uncertainty of the cross sections arises from the systematic errors in the detection efficiencies (5%) and the integrated luminosity (3%).

For the reaction (4.1) it is possible to find the interference phase θ_ϱ if one compares the results from Table 2 and the data which have been obtained for the decay $\varrho^- \to \pi^-\gamma$ [18—19] of its charged isotopic partner. If the interference phase θ_ϱ is equal to 165°, then the difference between $\Gamma(\varrho^- \to \pi^-\gamma)$ [19] and $\Gamma(\varrho^0 \to \pi^0\gamma)$ found from our data is about five standard deviations. On the other hand, if the phase is equal to −5°, then the widths found in these experiments are consistent. Therefore we will use the following value of the phase:

$$\theta_\varrho = (-5 \pm 6)°.$$

The fit of the data for the process (4.2) was also performed with two values of the phase θ_ϱ. As free parameters we have chosen the cross sections $\sigma_0(\omega \to \eta\gamma)$, $\sigma_0(\varrho \to \eta\gamma)$. A systematic error of the results presented in Table 3 is negligible.

Table 3

Values of the Cross Sections of the Reaction $e^+e^- \to \varrho, \omega \to \eta\gamma$.

Parametrs of the fit	$\theta_\varrho = 0°$	$\theta_\varrho = 180°$
$\sigma_0(\omega \to \eta\gamma)$ nb	$0.6^{+1.5}_{-0.6}$	3.4 ± 1.5
$\sigma_0(\varrho \to \eta\gamma)$ nb	$0.5^{+0.5}_{-0.4}$	0.9 ± 0.6
χ^2/n_D	4/9	6/9

5. REACTION $e^+e^- \to \omega \to \pi^0\pi^0\gamma$

To determine with high precision ϱ- and ω-meson parameters one should measure their rare neutral decay modes. In this chapter we describe a search for the process

$$e^+e^- \to \omega \to \pi^0\pi^0\gamma. \tag{5.1}$$

Two mechanisms can result in such a final state. The first is the reaction $\omega \to \varrho\pi \to \pi^0\pi^0\gamma$ with the usual radiative decay of the ϱ-meson [20]. Estimation shows that its probability is about 10^{-4}. Another possible mechanism is the electric dipole transition $\omega \to S\gamma$ where S is a scalar or tensor state ($S^*, \varepsilon, f, \ldots$) decaying into $2\pi^0$. Theoretical predictions for its probability are rather vague [15, 21] and vary from 10^{-2} to 10^{-5}. Experimentally electric dipole transitions between the resonances consisting of light quarks have not yet been observed.

Earlier we have studied the final state (5.1) at $2E > 1$ GeV [10]. Similar to that study, five-photon events, which had two π^0-mesons, with energy momentum balance were selected. Under such selection criteria no events have been found in the energy range of the ω-meson. From the detection efficiency of 2.2% the following upper limit for the branching ratio is obtained:

$$B(\omega \to \pi^0\pi^0\gamma) < 5 \cdot 10^{-4}. \tag{5.2}$$

This value is by a factor of 20 better than the table value [2] and does not show notable increase of the decay probability due to the final state interaction predicted in [15, 21].

6. PROCESS $e^+e^- \to \eta\gamma \to \pi^0\pi^0\pi^0\gamma$

As shown in previous chapter, no events of the reaction $e^+e^- \to \pi^0\pi^0\gamma$ were observed. Thus multiphoton events in this energy range must be mainly due to the process

$$e^+e^- \to \eta\gamma \to \pi^0\pi^0\pi^0\gamma\ . \tag{6.1}$$

A multiphoton final state is more convenient for the study of the decay ϱ,ω→ηγ than a three-photon one, because in this case the background level is much lower. To study this reaction events were

selected with four or more detected photons. To suppress the background due to cosmic particles and beam-gas we required a transverse momentum to be less than $0.2E$. Some photons escape detection, therefore only those events were selected, in which the energy deposition in the calorimeter was from $1.0E$ to $1.6E$.

A photon with the highest energy in (6.1) is the recoil photon. In Fig. 10,*a* we present a spectrum of recoil masses for a photon with the highest energy in events with five or more photons. A clear peak at the η-meson mass shows that the background is negligible. The background for four-photon events (Fig. 10,*b*) is due to the contribution of the process

$$e^+e^- \to 4\gamma \quad \text{(QED)}. \tag{6.2}$$

The observed number of events in Figs. 10,*a*,*b* is consistent with the expected contribution from the processes (6.1),(6.2). The presented spectra are well described by the simulation of these processes. Therefore we further use both four- and five-photon events. The detection efficiency is 4.5%.

In Fig. 11 the energy dependence of the visible cross section is shown for events with a η-meson. It was approximated by the sum of (6.1) and (6.2). For the cross section (6.1) the expression (4.6) has been used in which radiative corrections and the Φ-meson contribution [9] were taken into account, whereas the cross section (6.2) was calculated according to Ref. [22]. During the fit the cross sections $\sigma_0(\omega\to\eta\gamma)$ and $\sigma_0(\varrho\to\eta\gamma)$ were determined. The relative interference phases and the total width of the ω-meson (2.3) obtained in our work were fixed. If the phase values are taken from the quark model [1] ($\theta_\varrho=0°$, $\theta_\Phi=180°$), then the following values are obtained for the cross section:

$$\sigma_0(e^+e^-\to\omega\to\eta\gamma) = (0.9^{+0.7}_{-0.5})\ \text{nb}, \tag{6.3}$$

$$\sigma_0(e^+e^-\to\varrho\to\eta\gamma) = (0.5\pm0.2)\ \text{nb}.$$

These values agree with the results of the single previous measurement [23]. Note that a satisfactory χ^2 can be obtained in the fit with $\theta_\varrho=180°$. In this case, similar to Ref. [23], the cross section of the process (6.1) is by an order of magnitude larger:

$$\sigma_0(e^+e^-\to\omega\to\eta\gamma) = (7.3\pm1.2)\ \text{nb}, \tag{6.4}$$

$$\sigma_0(e^+e^-\to\varrho\to\eta\gamma) = (0.8\pm0.3)\ \text{nb}.$$

7. DISCUSSION

One of the most interesting results of this work is the measurement of the total width of the ω-meson. The values of the width obtained from the 3π and $\pi^0\gamma$ final states are consistent. Further we use the value (2.3) having a higher statistical accuracy.

This value is by four standard deviations lower than the table value (9.9±0.3) MeV [2] obtained by averaging the large number of measurements. Most of them were performed in hadronic reactions like $\pi^-p\to\omega n$. e^+e^--collisions provide the best conditions for such measurements, however, the accuracy in previous studies was low, about 1 MeV. A considerable increase in the accuracy attained in this work is due mainly to the high integrated luminosity. Processing of the second scan will check the correctness of (2.3).

From the value of the total width and the cross section in the peak one can calculate the branching ratios and partial widths for decays $\omega\to3\pi$, $\pi^0\gamma$, e^+e^-. The total cross section of the ω-meson production can be written as

$$\sigma_0(\omega\to\text{tot}) = \frac{\sigma_0(\omega\to3\pi)+\sigma_0(\omega\to\pi^0\gamma)}{1-\text{B}(\omega\to\pi^+\pi^-)} = (1718\pm126)\ \text{nb},$$

where we took into account only the decay modes with high enough branching fractions: $\omega\to3\pi$, $\pi^0\gamma$, $\pi^+\pi^-$. Here and below the error includes statisical and systematic uncertainties. From the total cross section one obtains the decay parameters:

$$\text{B}(\omega\to3\pi) = \sigma_0(\omega\to3\pi)/\sigma_0(\omega\to\text{tot}) = 0.896\pm0.008,$$

$$\text{B}(\omega\to\pi^0\gamma) = \sigma_0(\omega\to\pi^0\gamma)/\sigma_0(\omega\to\text{tot}) = 0.090\pm0.008,$$

$$\text{B}(\omega\to e^+e^-) = \frac{M_\omega^2}{12\pi}\cdot\sigma_0(\omega\to\text{tot}) = (7.2\pm0.5)\cdot10^{-5},$$

$$\Gamma(\omega\to3\pi) = (7.57\pm0.14)\ \text{MeV},$$

$$\Gamma(\omega\to\pi^0\gamma) = (757\pm69)\ \text{keV},$$

$$\Gamma(\omega\to e^+e^-) = (0.61\pm0.04)\ \text{keV}.$$

The obtained values of the branching ratios for the decays $\omega\to3\pi$, $\omega\to\pi^0\gamma$ do not differ from those in the table [2]. However, their partial widths are by 15% smaller due to a smaller total width. The leptonic width of the ω-meson and the branching ratio for the decay $\omega\to e^+e^-$ are in satisfactory agreement with the table values.

Using the table values of the total and leptonic width of the ϱ-meson as well as the peak cross section of the process $\varrho\to\pi^0\gamma$ one can calculate its branching ratio and partial width:

$$B(\varrho\to\pi^0\gamma)=(7.9\pm3.5)\cdot10^{-4},$$

$$\Gamma(\varrho\to\pi^0\gamma)=(122\pm54)\ \text{keV}.$$

As noted earlier, this value is consistent with the result of the measurement for the charged ϱ^--meson (Table 5).

In Table 4 our results on the decays $\omega,\varrho\to\eta\gamma$ are presented. The values of the branching ratio obtained from different decay modes of the η-meson: $\eta\to2\gamma$ and $\eta\to6\gamma$ agree with each other and their average value does not contradict the single previous measurement [23]. The branching ratios are given for two values of the interference phase $\theta_\varrho=0°$ and $\theta_\varrho=180°$, however, we use the value corresponding to $\theta_\varrho=0°$ predicted by the quark model [1].

Table 4

Branching Ratios of the Decays $\varrho\to\eta\gamma$, $\omega\to\eta\gamma$ for two values of the $\varrho-\omega$ interference phase 0° and 180°.

Branching ratio	Θ_ϱ, deg	$\eta\to2\gamma$	$\eta\to3\pi\to6\gamma$	Average value
$B(\omega\to\eta\gamma)\cdot10^4$	0	$3.2^{+8.0}_{-3.2}$	$5.6^{+4.4}_{-3.1}$	$4.6^{+3.8}_{-2.2}$
	180	18 ± 8	45 ± 8	32 ± 6
$B(\varrho\to\eta\gamma)\cdot10^4$	0	$4.4^{+4.4}_{-3.5}$	4.6 ± 1.9	4.5 ± 1.7
	180	7.9 ± 5.3	7.4 ± 2.4	7.5 ± 2.2

The obtained results on partial decay widths of the ϱ-, ω-mesons radiative decays as well as our previous results [9] are presented in Table 5. Also shown there are the table data [2] as well as the quark model predictions [1, 4, 24, 25]. In this model the width of the radiative decay has the form [24]:

$$\Gamma=\frac{4}{3}\omega^3|M_{VP}|^2,$$

where $\omega=\dfrac{M_V^2-M_P^2}{2M_V}$ is the photon energy, $M_{VP}=(q_1\mu_1+q_2\mu_2)I_{VP}$ is the transition matrix element, $q_{1,2}$ are quark charges, $\mu_{1,2}$ are their magnetic momenta, I_{VP} are overlapping integrals for wave functions. The ratio of the overlapping integrals for different decays is assumed to be unity. The quark magnetic moments are assumed to be different: $\mu_d/\mu_u=1.05$, $\mu_s/\mu_u=0.66$. The mixing angles are taken to be not ideal $\alpha_V=3.7°$, $\alpha_P=43.5°$ [2]. Using assumptions above and the width $\Gamma(\omega\to\pi^0\gamma)$ measured in this work one can calculate the widths of the other decays.

Table 5

Partial Widths of Radiative Decays

Decay $V\to P\gamma$	Quark model Γ, keV	Our results Γ, keV	Particle Data Group (1984) Γ, keV
$\omega\to\pi^0\gamma$	757 ± 69	757 ± 69	860 ± 50
$\varrho\to\pi^0\gamma$	70 ± 7	122 ± 54	71 ± 8
$\omega\to\eta\gamma$	4.4 ± 0.5	$3.9^{+3.2}_{-1.8}$	$3.0^{+2.5}_{-1.8}$
$\varrho\to\eta\gamma$	47 ± 5	69 ± 26	55 ± 14
$\Phi\to\eta\gamma$	67 ± 7	55 ± 3	51 ± 8
$\Phi\to\pi^0\gamma$	7.3 ± 0.7	5.5 ± 0.6	5.9 ± 2.1
$\Phi\to\eta'\gamma$	0.23 ± 0.03	<0.84	—

The data presented in Table 5 show that the difference between the quark model calculations and the values obtained is as a rule not larger than two standard deviations for all the decays. Thus the quark model successfully describes the radiative decays of ϱ, ω and Φ-mesons.

Using the data of the Neutral Detector one can obtain the parameters of the quark model itself. Similar to [9] one calculates

$$\Gamma(\Phi\to\pi^0\gamma)/\Gamma(\omega\to\pi^0\gamma)=(7.3\pm1.0)\cdot10^{-3},$$

$$\Gamma(\varrho\to\eta\gamma)/\Gamma(\omega\to\pi^0\gamma)=(9.0\pm3.5)\cdot10^{-2},$$

$$\Gamma(\Phi\to\eta\gamma)/\Gamma(\omega\to\pi^0\gamma)=(7.3\pm0.8)\cdot10^{-2}.$$

From these values one can obtain the mixing angles:

$$\alpha_v=(3.2\pm0.2)°,$$

$$\alpha_p=(-59\pm17)°,$$

as well as the ratio of the magnetic moments for *s*- and *u*-quark:

$\mu_s/\mu_u = 0.60 \pm 0.03$.

The values of the mixing angles coincide within the errors with the table data obtained using the quadratic mass formula. The ratio of the magnetic moments for *s*- and *u*-quark is close to the value 0.66 obtained from the magnetic moments of baryons.

In conclusion we should like to note that presented results are preliminary. Data on the radiative decays of the ϱ-meson have been obtained in a small energy range. Therefore the reliability and accuracy of the measurements will be improved during the data processing of a scan in a broad energy range.

REFERENCES

1. *P.J. O'Donnel*, Rev. Mod. Phys. 53 (1981) 673.
2. Review of Particle Properties. Particle Data Group, 1984.
3. *J. Keine et al.*, Phys. Rev. D14 (1976) 28.
4. *T. Oshima*, Phys. Rev. D22 (1980) 707.
5. *D. Benaksas et al.*, Phys. Lett. 42B (1972) 511.
6. *G.M. Tumaikin*, Proceedings of the 10-th International Conference on High Energy Particle Accelerators, Serpukhov, 1977, v.1, p.443.
7. *V.V. Anashin et al.*, Preprint INP 84-123. Novosibirsk, 1984.
8. *V.B. Golubev et al.*, Nucl. Instr. and Methods 227 (1984) 467.
9. *V.P. Druzhinin et al.*, Phys. Lett. 144B (1984) 136.
10. *V.B. Golubev et al.*, Yadernaya Fizika 41 (1985) 1176,
    V.P. Druzhinin et al., Preprint INP 84-93. Novosibirsk, 1984,
    S.I. Dolinsky et al., Preprint INP 85-98. Novosibirsk, 1985,
    S.I. Dolinsky et al., Preprint INP 86-69. Novosibirsk, 1986.
11. *N.N. Achasov, N.M. Budnev et al.*, Yadernaya Fizika 23 (1976) 616.
12. *E.A. Kuraev, V.S. Fadin*, Yadernaya Fizika 41 (1985) 733.
13. *P. Singer*, Phys. Rev. 130 (1963) 2441, 161 (1967) 1694.
14. *V.N. Baier, V.A. Khoze*, ZhETF 48 (1965) 1708.
15. *S.M. Renard*, Nuovo Cimento 62A (1969) 475.
16. *M.J. Creutz, M.B. Einhorn*, Phys. Rev. D1 (1970) 2537.
17. *V.B. Golubev et al.*, Report at the III-rd Ipternational Conference on Instrumentation for Colliding Beam Physics. Novosibirsk, USSR, 1984.
18. *B. Gobby et al.*, Phys. Rev. Lett. 33 (1974) 1450.
19. *T. Jensen et al.*, Phys. Rev. D27 (1983) 26.
20. *P. Singer*, Phys. Rev. 128 (1962) 2789.
21. *N. Levi and P. Singer*, Phys. Rev. D3 (1971) 2134.
    J. Yellin, Phys: Rev. 147 (1966) 1080.
22. *F.A. Berends et al.*, Nucl. Phys. B239 (1984) 395.
23. *D.E. Andrews et al.*, Phys. Rev. Lett. 38 (1977) 198.
24. *Ya.I. Azimov*, Preprint LINP 819 (Leningrad, 1982).
25. *D.A. Geffen and W. Wilson*, Phys. Rev. Lett. 44 (1980) 370.

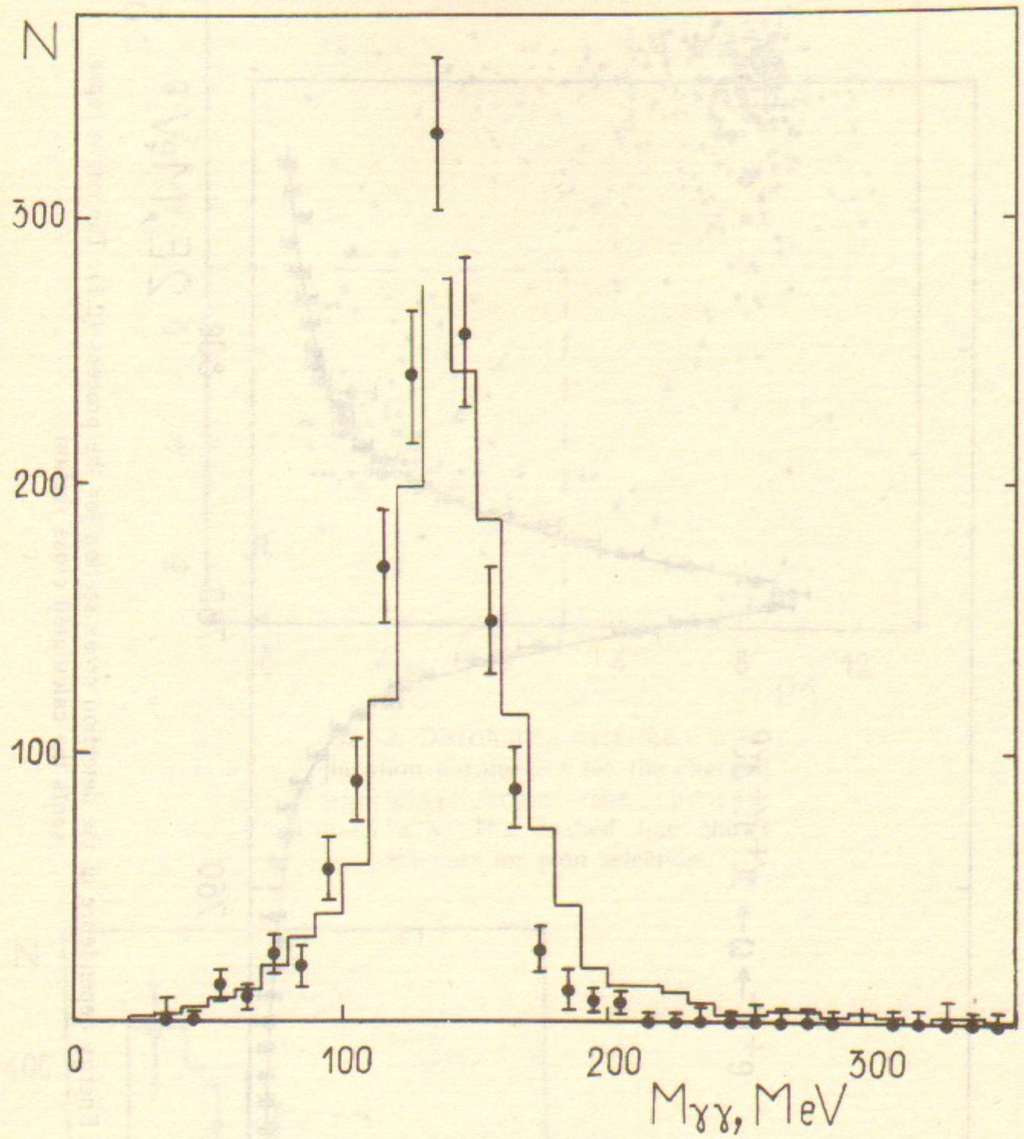

Fig. 1. Two photon invariant mass distribution for $\pi^+\pi^-\pi^0$ events at the energy $2E = 782$ MeV. Histogram — experiment, points — Monte-Carlo simulation.

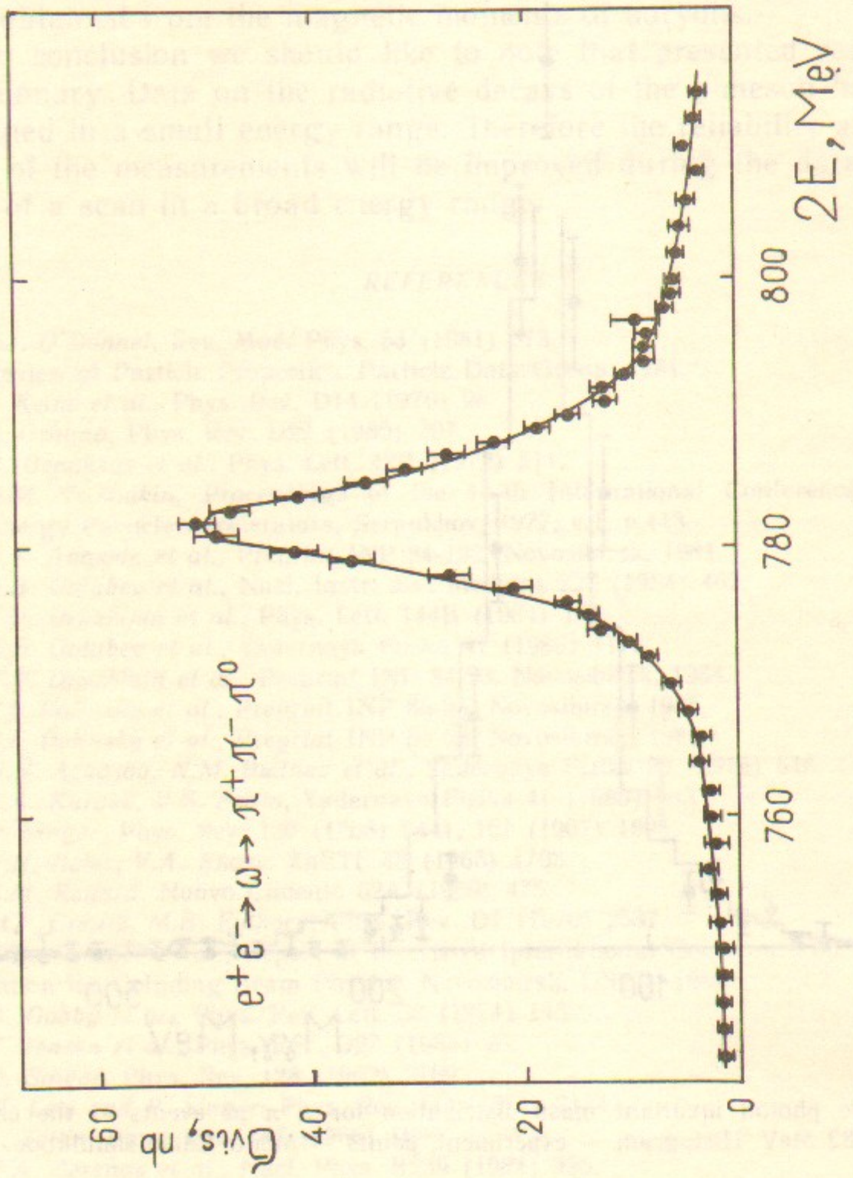

Fig. 2. Energy dependence of the detection cross section for the process (2.1). The curve represents the calculated cross section.

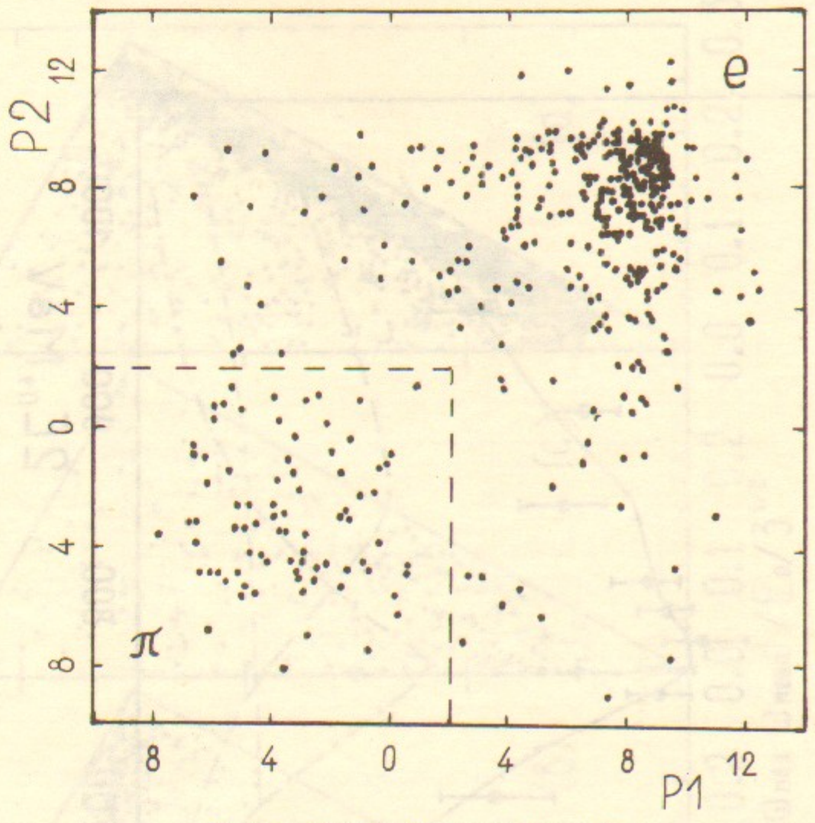

Fig. 3. Distribution over the e/π-separation parameters for the charged particles from the process $\varrho \to \pi^+\pi^-\gamma$. The dashed line shows the cuts for pion selection.

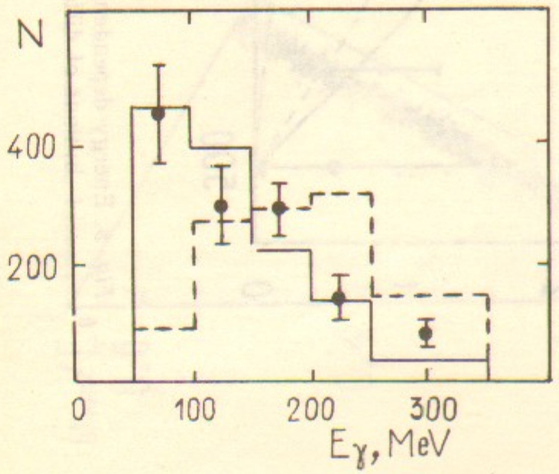

Fig. 4. Energy spectrum of the photon for selected events of $\varrho \to \pi^+\pi^-\gamma$ decay — points. Histogram — simulation of bremsstrahlug mechanism. Dashed line — decay through the scalar resonance $\varepsilon(700)$.

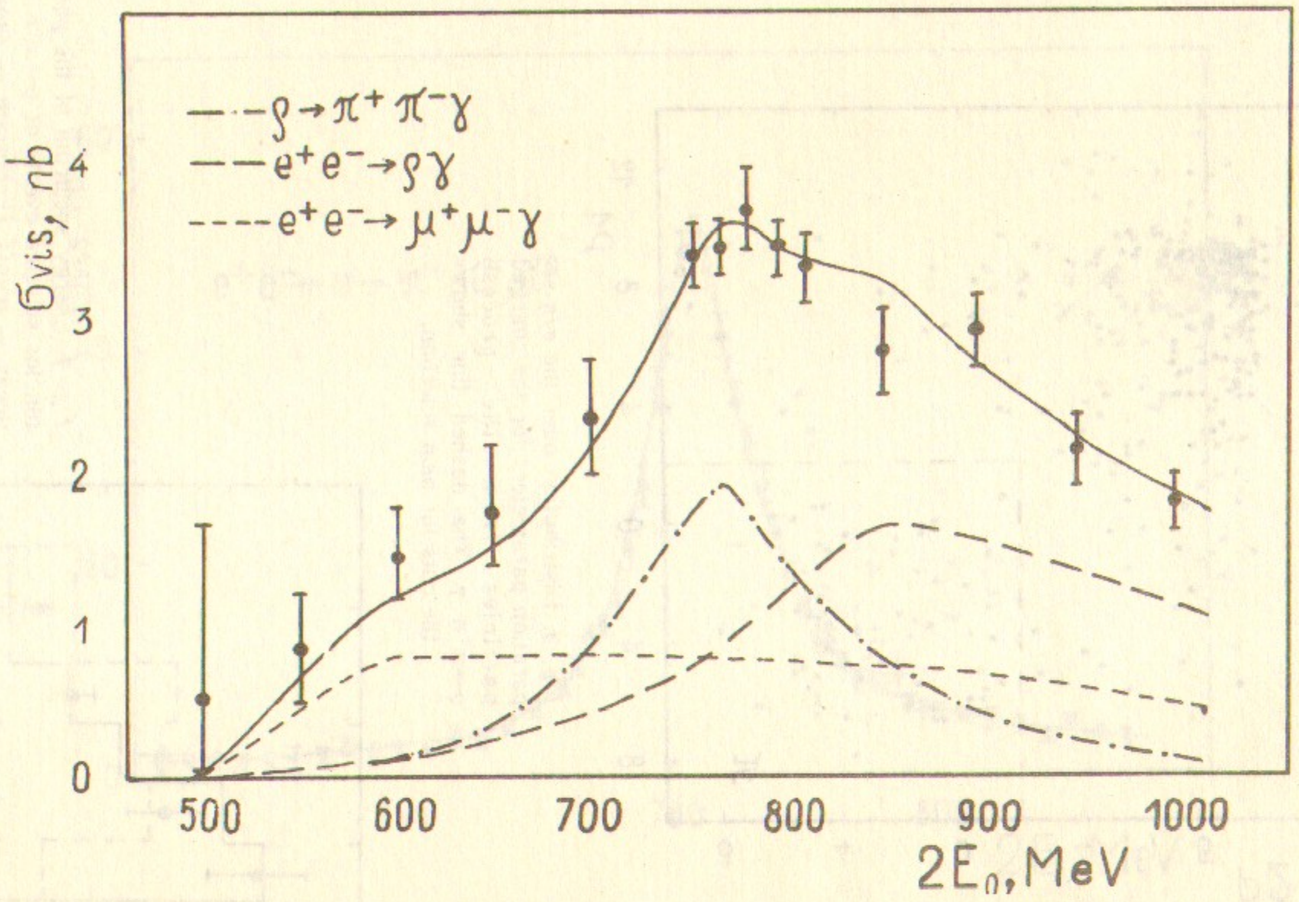

Fig. 5. Energy dependence of the detection cross section for selected events $\pi^+\pi^-\gamma$. The contributions of different processes and a sum of their cross sections are shown.

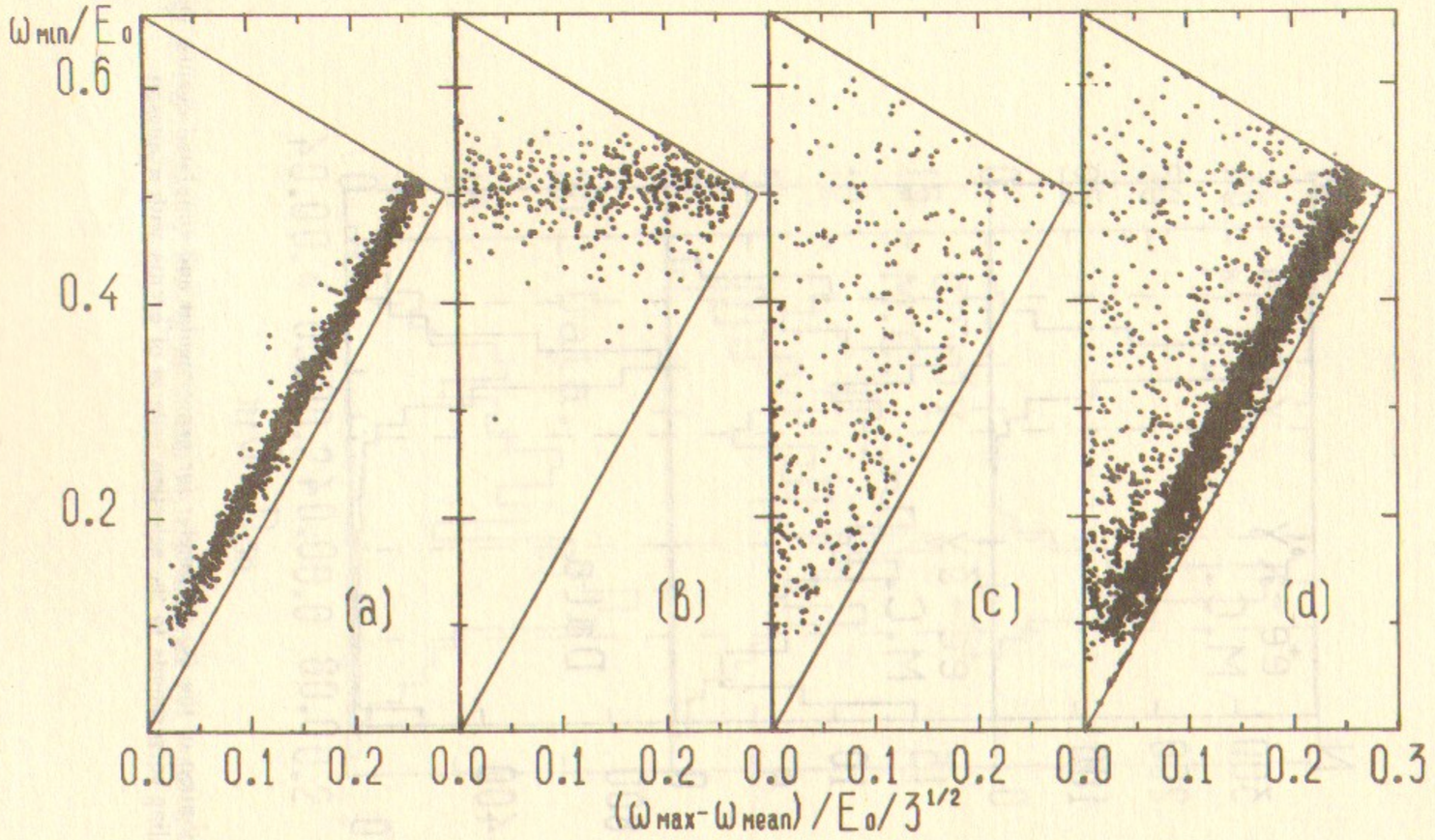

Fig. 6. Dalitz plots for three photon final state:
a, *b*, *c*—simulation of the process $e^+e^-\to\pi^0\gamma$, $\eta\gamma$, 3γ correspondingly, *d*—experimental data.

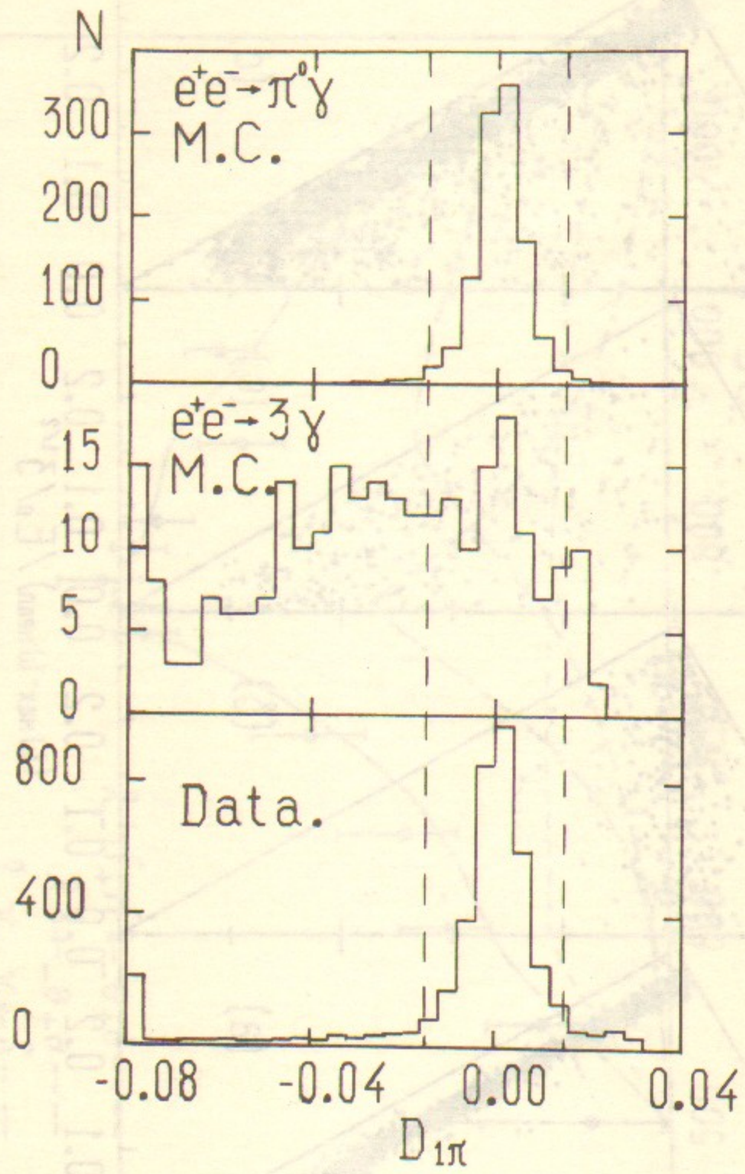

Fig. 7. Distribution of the $D_{1\pi}$ parameter for experimental and simulated events. Dashed line corresponds to the selection criteria of events with π^0-meson.

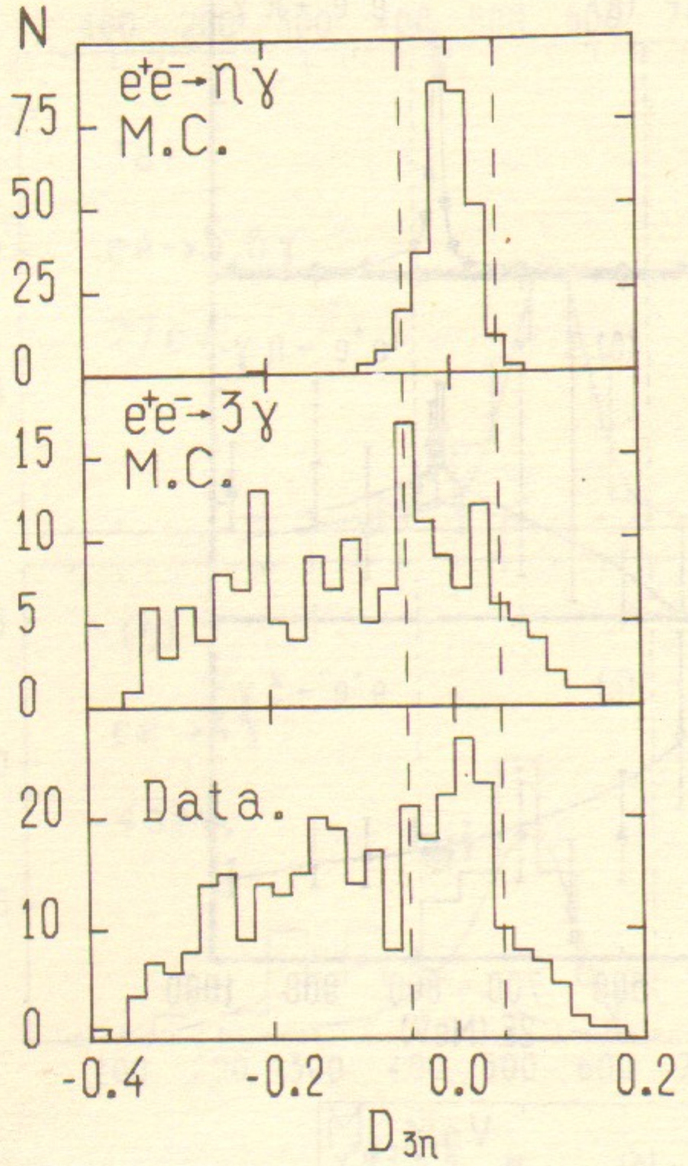

Fig. 8. Distribution of the $D_{3\eta}$ parameter for experimental and simulated events. Dashed line corresponds to the selection criteria of events with η-meson.

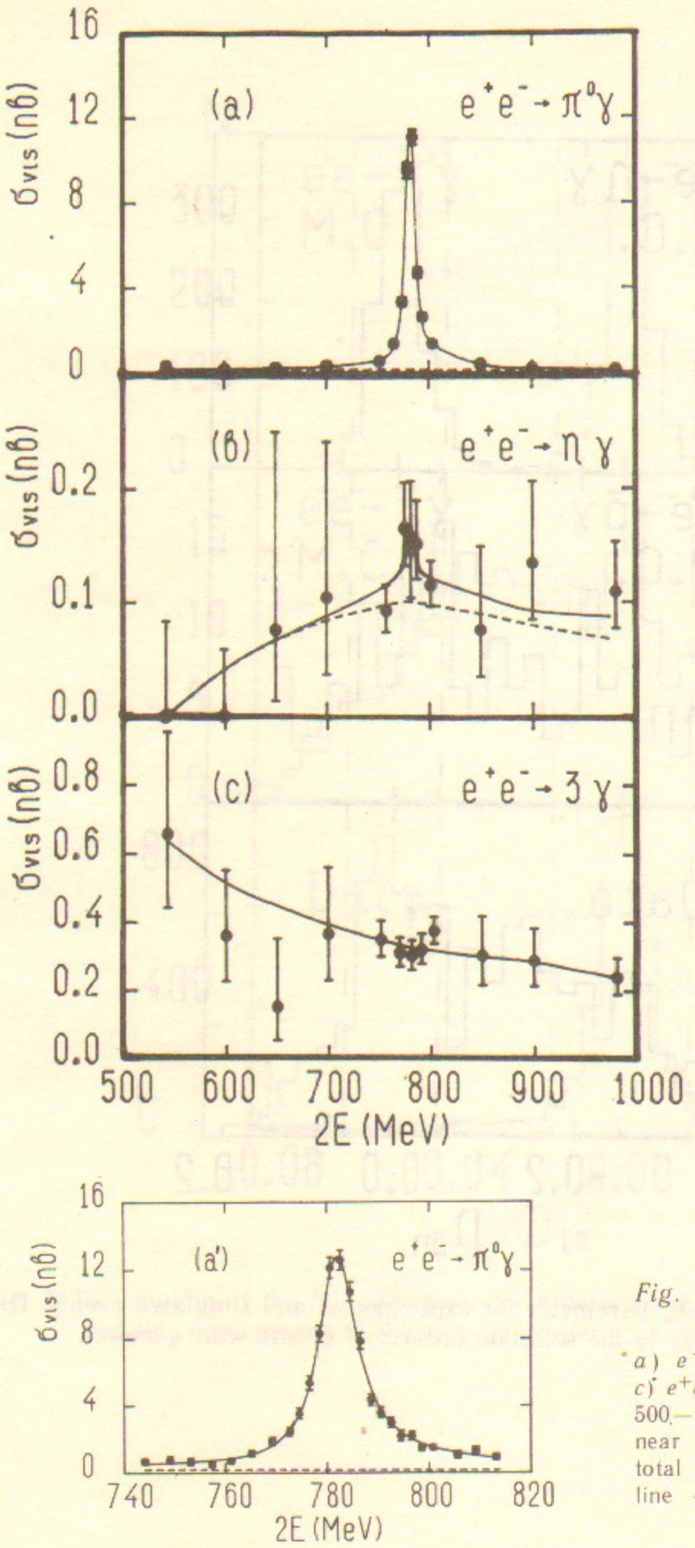

Fig. 9. Detection cross section for the process:

a) $e^+e^- \to \pi^0\gamma$, *b*) $e^+e^- \to \eta\gamma$, *c*) $e^+e^- \to 3\gamma$, in the energy range 500—1000 MeV; *a'*) $-e^+e^- \to \pi^0\gamma$ — near ω-meson mass. Solid curve — total detection cross section, dashed line — contribution of the process $e^+e^- \to 3\gamma$ (QED).

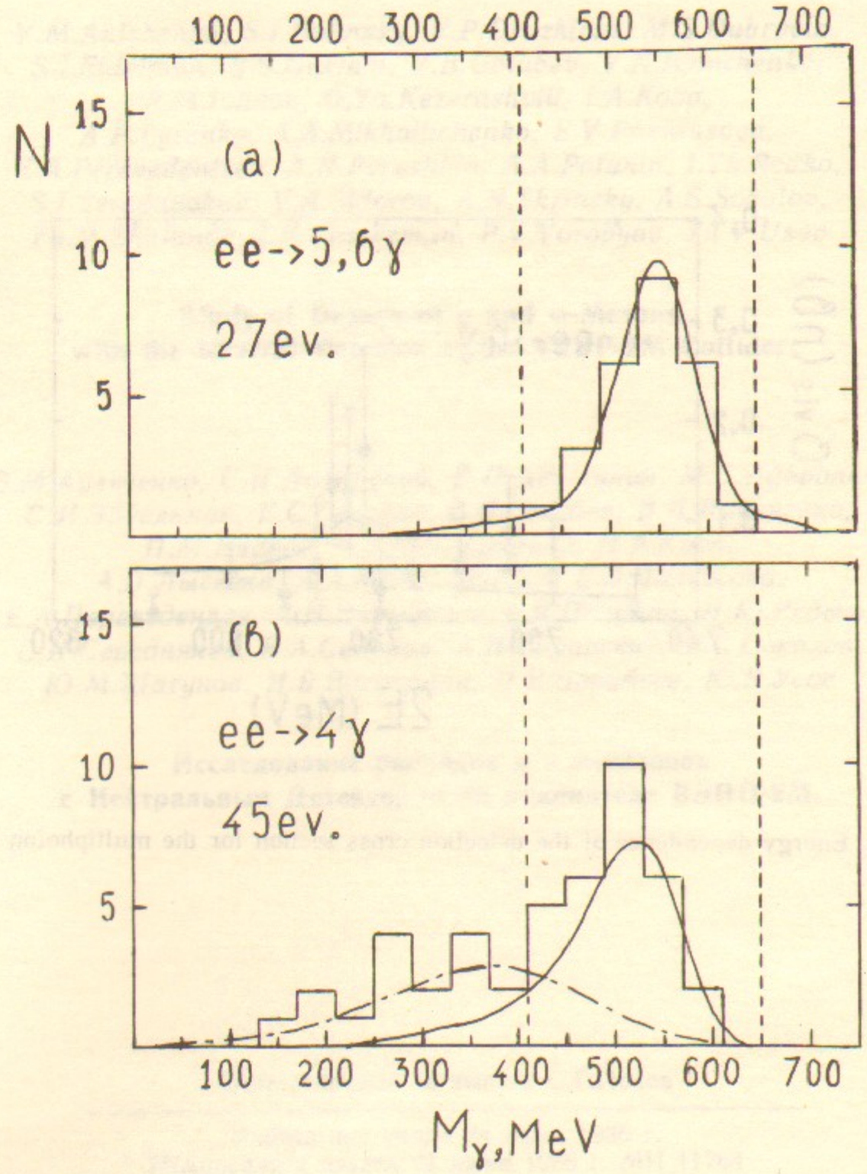

Fig. 10. Recoil mass spectrum for the maximum energy photon in multiphoton events. Histogram—experiment, solid line—simulation of the process $e^+e^- \to \eta\gamma$, dashed-dotted line—simulation of the process $e^+e^- \to 4\gamma$, dashed line corresponds to the selection criteria of events with η-meson.

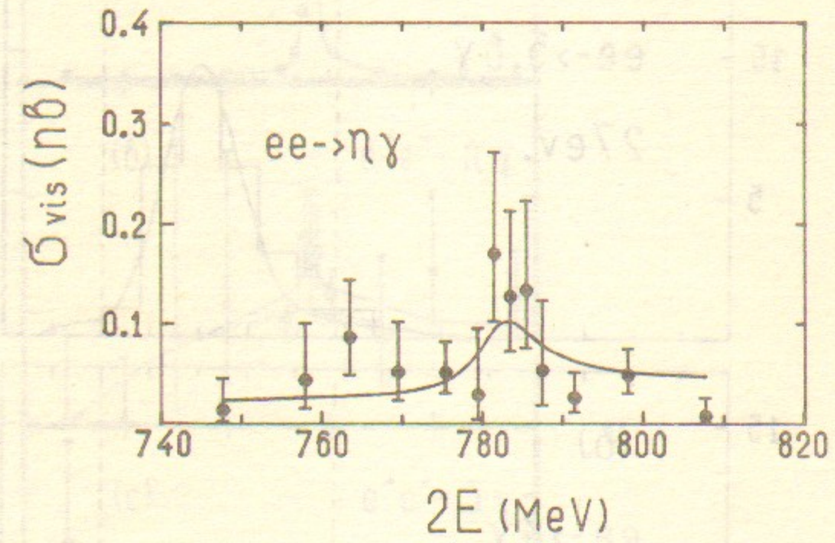

Fig. 11. Energy dependence of the detection cross section for the multiphoton events.

V.M.Aulchenko, S.I.Dolinsky, V.P.Druzhinin, M.S.Dubrovin, S.I.Eidelman, E.S.Gluskin, V.B.Golubev, V.N.Ivanchenko, P.M.Ivanov, G.Ya.Kezerashvili, I.A.Koop, A.P.Lysenko, A.A.Mikhailichenko, E.V.Pakhtusova, E.A.Perevedentsev, A.N.Peryshkin, A.A.Polunin, I.Yu.Redko, S.I.Serednyakov, V.A.Sidorov, A.N.Skrinsky, A.S.Sokolov, Yu.M.Shatunov, I.B.Vasserman, P.V.Vorobyov, Yu.V.Usov

Study of Desays of ϱ and ω-Mesons with the Neutral Detector at the VEPP-2M Collider

В.М.Аульченко, С.И.Долинский, В.П.Дружинин, М.С.Дубровин, С.И.Эйдельман, Е.С.Глускин, В.Б.Голубев, В.Н.Иванченко, П.М.Иванов, Г.Я.Кезерашвили, И.А.Кооп, А.П.Лысенко, А.А.Михайличенко, Е.В.Пахтусова, Е.А.Переведенцев, А.Н.Перышкин, А.А.Полунин, И.Ю.Редько, С.И.Середняков, В.А.Сидоров, А.Н.Скринский, А.С.Соколов, Ю.М.Шатунов, И.Б.Вассерман, П.В.Воробьев, Ю.В.Усов

Исследование распадов ϱ и ω-мезонов с Нейтральным Детектором на накопителе ВЭПП-2М.

Ответственный за выпуск С.Г.Попов

Работа поступила 24 июня 1986 г.
Подписано к печати 27 июня 1986 г. МН 11764
Формат бумаги 60×90 1/16 Объем 2,9 печ.л., 2,7 уч.-изд.л.
Тираж 150 экз. Бесплатно. Заказ № 105

Набрано в автоматизированной системе на базе фотонаборного автомата ФА1000 и ЭВМ «Электроника» и отпечатано на ротапринте Института ядерной физики СО АН СССР.
Новосибирск, 630090, пр. академика Лаврентьева, 11.